A New Design Paradigm for Smart Windows: Photocurable Polymers for Quasi-Solid Photoelectrochromic Devices with Excellent Long-Term Stability under Real Outdoor Operating Conditions

Federico Bella, George Leftheriotis,* Gianmarco Griffini, George Syrrokostas, Stefano Turri, Michael Grätzel, and Claudio Gerbaldi*

A new photoelectrochromic device (PECD) is presented in this work proposing the combination of a WO_3-based electrochromic device (ECD) and a polymer-based dye-sensitized solar cell (DSSC). In the newly designed architecture, a photocurable polymeric membrane is employed as quasi-solid electrolyte for both the ECD and the DSSC. In addition, a photocurable fl uoropolymeric system is incorporated as solution-processable external protective thin coating fi lm with easy-cleaning and UV-shielding functionali-ties. Such new polymer-based device assembly is characterized by excellent device operation with improved photocoloration effi ciency and switching ability compared with analogous PECDs based on standard liquid electrolyte systems. In addition, long-term (>2100 h) stability tests under continuous exposure to real outdoor conditions reveal the remarkable performance stability of this new quasi-solid PECD system, attributed to the protective action of the photo-curable fl uorinated coating that effectively prevents photochemical and physical degradation of the PECD components during operation. This fi rst example of quasi-solid PECD systems paves the way for a new generation of thermally, electrochemically, and photochemically stable polymer-based PECDs, and provides for the fi rst time a clear demonstration of their true potential as readily upscalable smart window components for energy-saving buildings.

1. Introduction

Smart windows are currently under intense investigation and thorough optimization in order to be effectively imple-mented in modern energy-saving buildings.[1] The possibility of altering the light transmission proper-ties of a window upon a voltage-, light-, or heat-induced external stimulus is a fundamental requirement to be pursued, and scientists are carefully investigating the quality, speed, and repeatability of the optical switching phenomenon. The resulting smart windows (often referred to as "building shells") offer several advan-tages if compared to traditional ones, with a neat money saving for air-conditioning, heating, lighting, and curtains.

Photoelectrochromic devices (PECDs) represent the most promising and fasci-nating technology for the realization of smart windows, and stem from the com-mingling of a dye-sensitized solar cell (DSSC) and an electrochromic device (ECD).[2] Among the few examples of cell architectures that have been proposed so far for PECDs, the most performing ones include a dye-covered nanostructured TiO_2layer deposited onto a porous WO_3 layer and a counter electrode constituted of a thin Pt fi lm; the space between the elec-trodes is typically fi lled with a I − /I 3 − -based liquid electrolyte containing Li + ions. Based on such a confi guration, the chem-isorbed dye molecules absorb photons upon illumination and inject electrons into the conduction band of the TiO 2 ; then, the electrons diffuse into the WO 3 layer. At the same time, Li + ions

Dr. F. Bella, Prof. C. Gerbaldi
GAME Lab, CHENERGY Group
Department of Applied Science and Technology—DISAT
Politecnico di Torino
CorsoDucadegliAbruzzi24, 10129 Turin, ItalyE-mail: federico.bella@polito.it
Dr. G. Leftheriotis, Dr. G. Syrrokostas
Energy and Environment Lab
PhysicsDepartment
University of Patras
26504 PanepistimioupoliPatron , Greece
E-mail: gleftther@physics.upatras.gr
Dr. G. Griffini, Prof. S. Turri
Department of Chemistry
Materials and Chemical Engineering "Giulio Natta",
Politecnico di Milano
PiazzaLeonardodaVinci32, 20133 Milan, Italy
Prof. M. Grätzel
Laboratory of Photonics and Interfaces
Institut des Sciences et Ingénierie Chimiques
Ecole Polytechnique Fédérale de Lausanne (EPFL)
Station3, CH-1015 Lausanne, Switzerland

intercalate into the WO_3, resulting in its switching from transparent to blue color, the latter lasting until the device is short-circuited or the irradiance is attenuated. Both DSSCs and ECDs have been deeply investigated during the last two decades, their properties being easily fi ne-tuned as required.[3] The hybrid device that results from their proper combination may combine dynamic solar control with power production, also allowing the achievement of a series of interesting new properties. First, thanks to the electrons produced by the DSSC, the ECD does not require an external power supply, which has often been a limiting factor for the widespread application of these devices. Second, PECD technology might ensure a commercial outlet to DSSCs in which their characteristics in terms of transparency, color tunability, cost, and ease of manufacture would result unmatched by other existing photovoltaic (PV) devices. Moreover, the speed of coloration and bleaching does not depend on the device area (differently from ECDs), but only on the internal electrical fi eld generated by the PV unit. Therefore, the speed of coloration obtained by small lab-scale samples is also applicable to large area windows, thus potentially speeding up the scale-up process for this technology. Recently, the electrical separation of solar cell and electrochromic elements in the same device has also been proposed, which led to a brand new research area, namely, photovoltachromics or energy-harvesting electrochromic windows.[4]

Being PECDs a relatively new technology, the scientific community has mainly focused on the investigation of its basic components. Photoanodes fabrication,[5] organic electrodes,[6] electrodes functionalization,[7] and hybrids with supercapacitors[8] have been recently proposed and thoroughly studied so far. Nevertheless, many important aspects still need to be carefully addressed in order to further improve the level of reliability, feasibility, and real implementability of this technology in the foreseeable future. In this context, the most critical point concerns the long-term stability of all the cell components. In particular, the volatility, photoinstability, corrosion, and leakage of the liquid electrolyte and the cleanliness of the PECD, especially considering the side exposed to the external environment, are the most critical factors that limit the real applicability of these systems. With regard to the electrolyte, only few alternatives to the standard liquid electrolyte have recently been proposed in an attempt to reduce the volatility of this component and potentially enhance the PECD lifetime. Hechavarría et al. formulated a viscous polymer electrolyte applying the sol-gel method to a mixture of poly(ethylene glycol) and titanium isopropoxide, followed by the addition of lithium iodide (LiI).[9] Wu et al. prepared a gel electrolyte by mixing succinonitrile, poly(vinylidenefluoride-*co*-hexafl uoropropylene), and propylene carbonate.[10] Several years ago, poly(ethylene glycol) dimethacrylate,[11] ormosilane networks,[12] and poly(3,4-ethylenedioxythiophene-*co*-styrenesulfonate)[7] were also introduced in PECDs in order to replace liquid electrolytes. However, two fundamental issues must be underlined after having examined the above-discussed state-of-the-art works. First, many of these polymer electrolytes are in fact viscous liquids and not self-standing solids. Therefore it is unlikely to foresee the absence of material loss and leakage paths with these systems on a long-term period (typically years) when employed in real PECD-based smart windows, especially in the presence of small sealing defects (almost unavoidable when considering the current fabrication processes for third-generation PV devices).[13] Moreover, when incorporated in smart window elements, the cleanliness of the external glass of the PECD (i.e., the one directly exposed to outdoor weathering and aging) represents a fundamental requirement that has never been investigated in the literature so far. Nevertheless, this aspect is essential to maintain the transparency of the device during operation as well as to avoid any inhibition of the TiO_2/dye-operated sunlight harvesting process resulting from the presence of dust or other contaminating particles.[14] Notably, to our knowledge none of the reports on (quasi)-solid PECDs showed a detailed aging test under real outdoor conditions (also in the presence of the UV component of sunlight), which is a fundamental investigation to be carried out for a hybrid organic/inorganic device conceived to be used as a smart window.

With the aim of addressing all of these issues, in this work we propose a polymer-based, easily-cleanable, and highly stable light-cured PECD. As sketched in **Scheme 1**, in our newly designed architecture a photocrosslinked polymer membrane behaves—at the same time—as quasi-solid electrolyte (after proper activation), source of both lithium and iodide ions, electrode separator, and 3D macromolecular cage for the effective

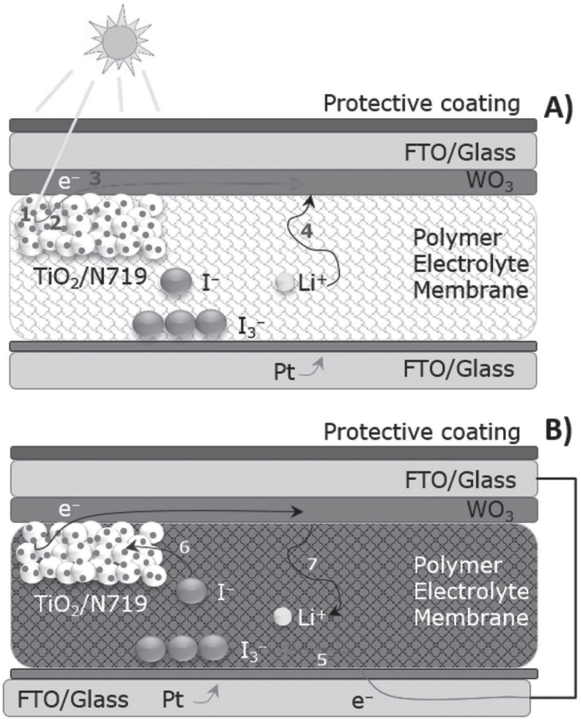

Scheme 1. Sketched architecture of the proposed quasi-solid polymeric PECD in its A) bleached and B) colored states, respectively. Device operation involves seven different processes: (1) absorption of photons by the N719 dye; (2) injection of electrons from the N719 dye into the TiO_2 electrode; (3) diffusion of electrons from the TiO_2 into the WO_3 layer; (4) intercalation of Li^+ ions into the WO_3 active material particles for charge equilibration, resulting in the coloration of the WO_3 film under open-circuit conditions; (5) under dark and short-circuit conditions, electrons reach the Pt layer at the counter electrode and reduce I_3^- to I^-; (6) I^- reduces the N719 dye molecules; and (7) Li^+ is transferred back to the electrolyte and the WO_3 film bleaches.

trapping of the redox couple upon operation time. Moreover, a few microns-thick fluoropolymeric fi lm deposited onto the external glass of the PECD acts as an easily cleanable and UV-blocking layer, by preventing the deposition of water and soil/dust particles onto it during outdoor operation and simultaneously protecting the organic components of the device from the harmful UV portion of the solar spectrum. All the macromolecular components presented herein are prepared by free-radical photopolymerization, which is an attractive technique for the design and straightforward preparation of polymer electrolytes and coatings, without resorting to the use of catalysts and/or external heat sources.[15] Both the newly developed materials and the quasi-solid PECD assembly were thoroughly characterized in terms of their chemical, thermal, morphological, and electro-optical properties. In addition to demonstrating excellent operation after in-lab assembly, the newly designed devices show exceptional stability during prolonged aging tests conducted under real outdoor weathering conditions.

2. Results and Discussion

The initial part of the work was focused on the preparation of the TiO_2/WO_3 electrodes. We fabricated optical quality WO_3 fi lms, having nearly 75% transmittance in the visible. Their thickness ranged from 400 to 600 nm, as measured ex situ by profi lometry. In **Figure1** A,B, scanning electron microscopy (SEM) images of the top and side view of the WO_3 films are shown. Films are composed by grains with size in the range of few hundreds of nanometers and have a porous structure, as it is evident also from the side view image. The packing density of the films was calculated to be around 0.805.[16] A TiO_2 film was deposited onto the bottom part of the WO_3 layer, in order to create a nanostructured electrode where dye molecules might be chemisorbed. The thickness of the TiO_2 films is equal to 12.5 ± 1 µm, as measured by profi lometry, and its morphology is shown in Figure 1C. Such a fi lm consists of nanoparticles with sizes around 20–25 nm, indicating the absence of aggregates in the precursor viscous paste solution. Further characterizations of the TiO_2/WO_3 electrode are given in Figures S1 and S2 in the Supporting Information.

PECDs are usually assembled with a liquid electrolyte, which does not guarantee suffi cient stability to the device so as to be used for the long-term 15–20 years of operational life typically required for smart window applications. As an alternative, a crosslinked polymer membrane can be prepared and used as quasi-solid electrolyte, source of redox mediator ions, separator for the electrodes, and 3D macromolecular cage for the effective trapping of the electrolyte components upon time.[17] In order to keep the fi nal device and fabrication costs as low as possible, it is highly desirable to make use of an economic, cheap, and eco-friendly technique to prepare such a polymer electrolyte. To this purpose, photopolymerization stands out as one of the most suitable techniques, mainly, because it does not require any harmful solvents, costly catalysts, and lengthy heating/cooling and purification procedures.[18] In order to prepare the photocrosslinked system, a dimethacrylic oligomer (i.e., bisphenol A ethoxylate dimethacrylate, BEMA) and a reactive diluent (poly(ethylene glycol) methyl ether methacrylate, PEGMA) bearing dangling

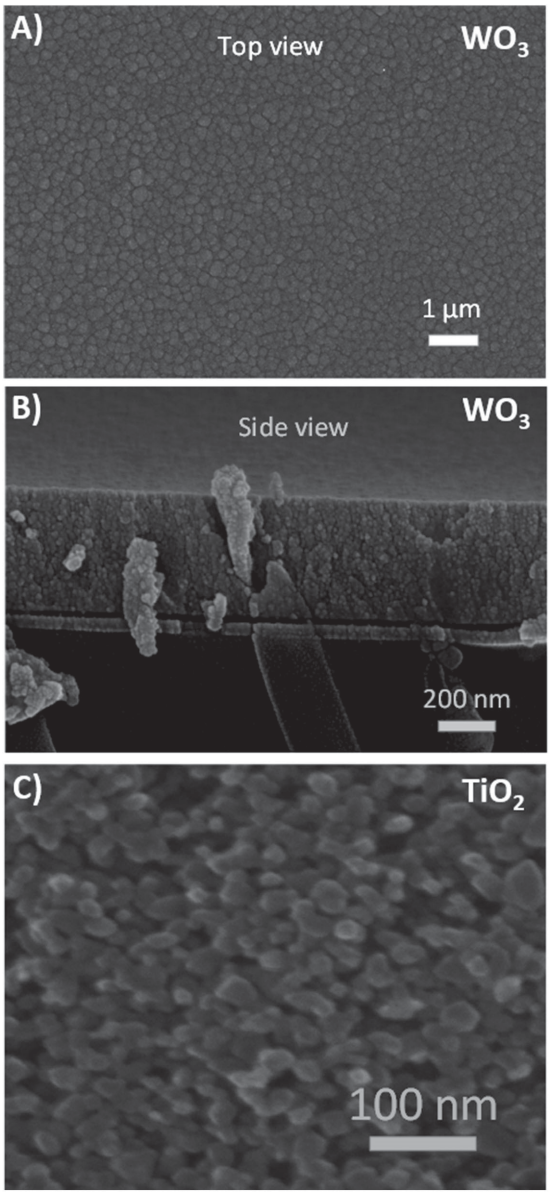

Figure 1. A) Top and B) side view SEM images of the WO_3 films prepared by e-beam evaporation. C) SEM image of the TiO_2 film grown on top of the WO_3 layer.

ethoxy groups were mixed together along with the addition of a free-radical photoinitiator (Irgacure 1173, 2 wt%). Being a dimethacrylate, BEMA readily undergoes crosslinking under UV light to form a solid 3D network; on the other hand, PEGMA is a monofunctional comonomer that allows the modification of the final characteristics of the macromolecular cage by lowering the glass transition temperature (T_g), reducing the crosslinking density and increasing the mobility of the lithium ions by coordinating with the –EtO– units of the pendant ethoxy groups.[17a,c] Moreover, the mixing of the two methacrylates with the photoinitiator is instantaneous and occurs at ambient conditions, thus leading to a ready-to-use reactive mixture.

UV-curable formulations were irradiated under UV light for 2 min between two UV-transparent glasses able to produce

a membrane with a thickness of 100 μm that can be easily detached for appropriate characterization. The kinetics of the UV-curing process was followed by real-time Fourier-transform infrared (RT-FTIR) spectroscopy, and the resulting conversion curve is shown in Figure S3 in the Supporting Information. A 100% fi nal conversion is reached in a few minutes, thus demonstrating the rapidity of such a light-induced polymerization process. This result appears particularly interesting if compared to the traditional solvent-based and time-consuming polymer electrolyte preparation procedures (e.g., solvent casting, melt fl ow, thermal processes) usually adopted for the fabrication of DSSCs and other electrochemical devices.[9–12] The gel content value (i.e., the percentage of polymeric matrix insoluble in chloroform) was found to be 99%, clearly indicating that the final UV-cured sample is a highly crosslinked thermoset material. After preliminary scanning and results evaluation, the combination of BEMA and PEGMA in the 30:70 ratio demonstrated to be the best formulation in terms of optimum chemical-physical, thermal, and electrochemical properties.

Soon after the photopolymerization process, the cross-linked solid polymer network was activated by soaking in a liquid electrolyte solution containing both lithium and iodide ions dissolved in acetonitrile. Interestingly, the resulting truly quasi-solid polymer electrolyte remains self-standing, nontacky, transparent, fl exible, and easy to handle as evidenced in the inset of **Figure2** B. To evaluate the mechanical stability of the polymeric electrolyte membrane, a bending test (50 cycles) was performed: the photopolymer electrolyte was found to be able to easily and reversibly withstand bending and rolling, down to a bending radius of 3 mm without compromising its overall mechanical integrity and elasticity. In addition, no electrolyte leakage was observed during bending. These results clearly evidence the truly quasi-solid nature of our newly designed polymer electrolyte system, which represents a significant improvement in terms of mechanical integrity and robustness compared to the liquid or viscous gel electrolytes typically presented in the literature for similar applications.[9]

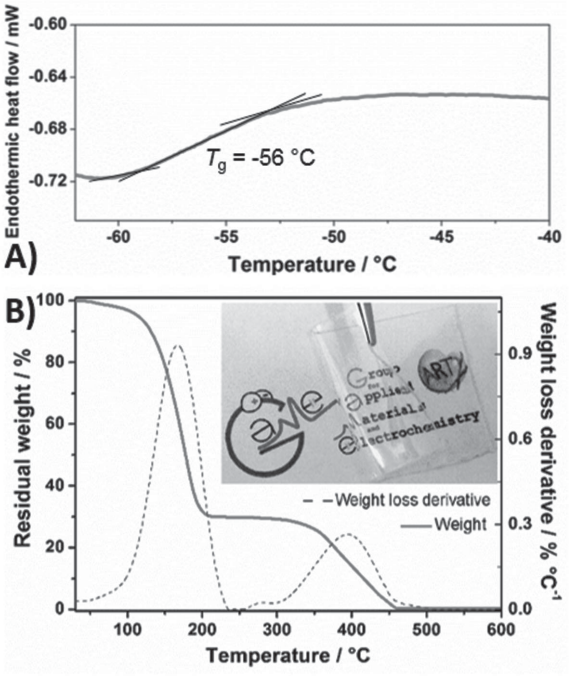

Figure 2. A) DSC traces of the photocured methacrylate-based polymer electrolyte membranes after the activation process performed by soaking it into an acetonitrile solution containing LiI 0.50 M, I_2 5.0×10^{3} M, and TBP 0.50 M. B) TGA thermogram of the same sample. Inset: Digital image of the activated sample after bending test (50 cycles).

The T_g of the activated polymer electrolyte membrane was analyzed by differential scanning calorimetry (DSC). The resulting curve is shown in Figure 2A. The T_g, defined as the midpoint of the heat capacity deflection observed in the DSC trace during the transition from glassy to rubbery state, is equal to −56 °C. Such a value both ensures the polymer electrolyte to be in the rubbery state at ambient conditions and guarantees the absence of phase transitions in the temperature range usually experienced by a PECD under real outdoor operational conditions. The thermal stability of the polymer electrolyte membrane was evaluated by means of thermogravimetric analysis (TGA) under flowing nitrogen, and the resulting curve is shown in Figure 2B. The activated photopolymer electrolyte shows a two-step degradation process, with two major well-defined weight loss events associated with the thermal stability of the materials used for the membrane preparation. The first degradation step (steep weight loss) occurs slightly above 100 °C and can be ascribed to the evaporation of acetonitrile solvent. The second step (at around 350 °C) is ascribed to the degradation of the methacrylate-based polymer network. Overall, as evidenced by the test, the proposed polymer electrolyte may guarantee safe practical operation of PECD systems in the temperature range between −50 and 100 °C.

A lab-scale PECD was assembled by placing the activated quasi-solid photopolymer electrolyte membrane between a front electrode (TiO_2/WO_3, where TiO_2 covers 15% of the total WO_3 area) and a counter electrode (planitized fluorine-doped tin oxide (FTO) glass). In such a device, the TiO_2 electrode was previously sensitized with the standard N719 dye, while the polymer membrane was activated by a 3 min soaking in an acetonitrile solution containing LiI 0.50 M, I_2 5.0×10^{-3} M, and 4-*tert*-butylpyridine (TBP) 0.50 M. After assembly, the processes of coloration and bleaching were studied by repeatedly irradiating the device in open-circuit conditions and keeping it short-circuited under dark, respectively. The device exhibits a fast coloration, i.e., its transmittance is nearly halved after only 8 s of illumination (see **Figure 3**A). Bleaching proceeds less rapidly (see Figure 3B and **Figure 4**A), but this is expected in the first coloring/bleaching cycle as the PECD has not yet reached its equilibrium. Indeed, 10–20 d are required after device assembly for the whole WO_3 surface to be fully wetted by the electrolyte. Such an "induction" period is normally found to be necessary before stabilization of device behavior.[19] Furthermore, it should be noted that, unlike displays, switchable windows do not need to exhibit fast coloration-bleaching transition, as the continuous modification of their transmittance might become a hindrance to the occupants of the building where they are installed.

A comparison with a corresponding liquid PECD is given in Figure 4B. The analysis of the photocoloration efficiency (PhCE) values clearly evidences the improved performance of the polymeric device, especially in the initial stages of the exposure. Overall, PhCE is larger during the initial stages and then

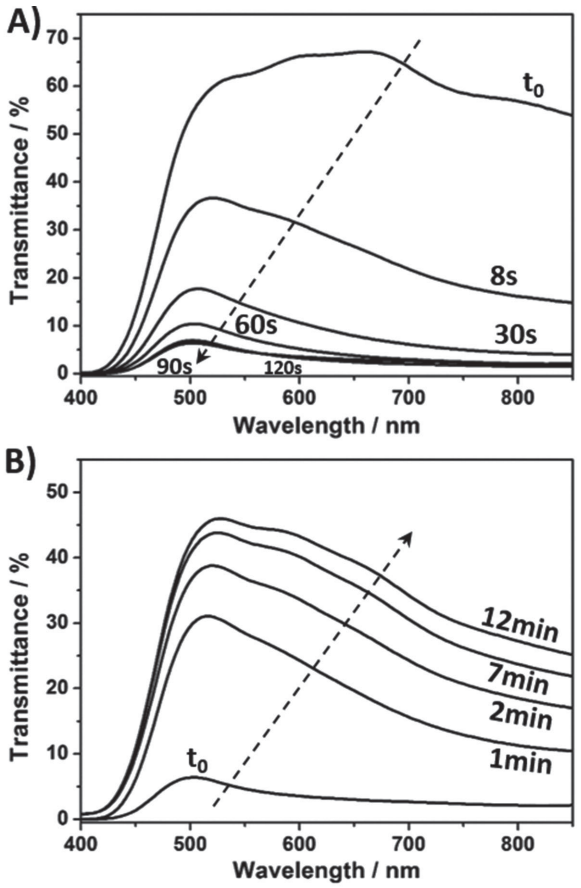

Figure 3. Transmittance spectra for quasi-solid PECD: A) coloration under 1000 W m^{-2} (AM 1.5G) illumination and B) bleaching under dark and short-circuit conditions.

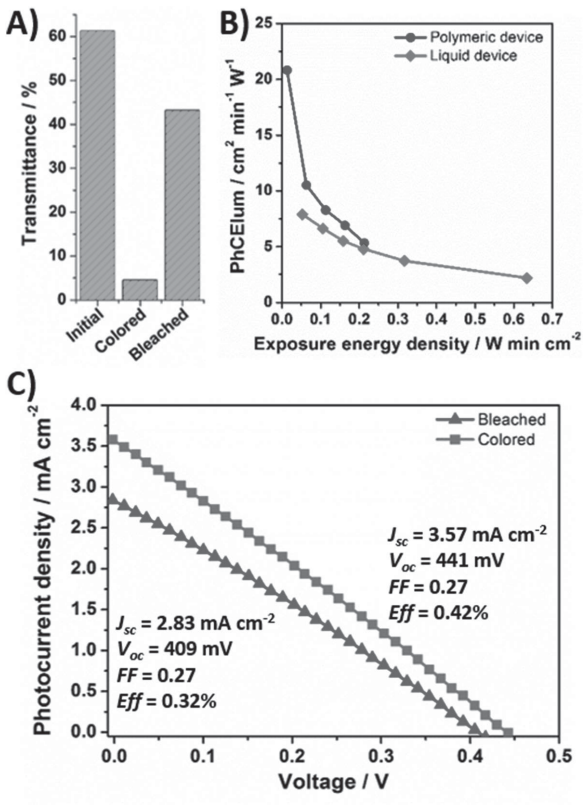

Figure 4. A) Variation of the luminous transmittance of the quasi-solid PECD, revealing initial partial reversibility. B) Photocoloration efficiency (PhCE) of polymeric and liquid PECDs. C) *J–V* curves of the polymeric PECD (area = 1.80 cm^2, irradiation intensity = 1 sun) before and after coloration.

decreases as the WO_3 film gets saturated by the Li^+ ions, as expected. The electrical characteristics of the DSSC fabricated onto the WO_3 layer are shown in Figure 4C. The *J–V* curves are acceptable taking into account the low annealing temperature of the TiO_2-based photoanode (100 °C), which was adopted to preserve the quality of the underlying WO_3 film. Furthermore, in order to improve PECD transmittance, less I_2 was added to the electrolyte ($[I_2] = 5 \times 10^{-3}$ M) in comparison with the standard concentration value usually adopted for DSSCs (50×10^{-3} M). Furthermore, the efficiency of the PV element increases when the measurement is carried out after coloration of the device, since the charge "stored" in the WO_3 active material particles is released and contributes to the total PV current generated.[19]

For smart window applications, the ability to preserve the cleanliness of the front electrode surface in PECDs during real outdoor operation is of paramount importance as the accumulation of dust, soil, or other external particles significantly affects the optical clarity and, thus, the long-term performance of the system. In addition, under outdoor conditions, PECDs are typically exposed to variable meteorological phenomena that may include rain, wind, snow, and icing, as well as the obvious action of the high-energy UV portion of the solar spectrum. All of these severe challenges for the long-term durability of the materials constituting the PECD stack require appropriate actions to enhance device lifetime. Rather surprisingly, the present literature seems to overlook this aspect as the vast majority of the works related to PECD stability mainly focuses on the evaluation of the "shelf-life" of the devices under dark conditions.[9,11,20] To our knowledge, no long-term studies on PECD operation under real outdoor conditions have been presented so far and no examples of potential strategies to enhance PECD outdoor lifetime have been proposed. To bridge this gap, we developed in this work a high-durability UV-curable protective coating (herein referred to as XL-coating), based on the combination of a UV-curable chloro-trifluoro-ethylene-vinyl-ether (UV-CTFEVE) polymeric binder recently developed in our laboratories[14,21] and a commercial difunctional methacrylic perfluoropolyether (PFPE) oligomer (Fluorolink MD700, from here on simply MD700). In this regard, it is well known that fluorinated polymers are characterized by excellent outdoor durability and their use in several technological fields has been demonstrated.[22]

To obtain the XL-coating, UV-CTFEVE was mixed with MD700 in the presence of a suitable free radical photoinitiator (Irgacure 1173, 3 wt%) and the spin-casted reactive precursor mixture was then exposed for 60 s to UV light under inert atmosphere. The addition of MD700 to UV-CTFEVE (their chemical structures are shown in the inset of **Figure 5**) is expected to enhance the hydrophobic character of the chlorofluorinated

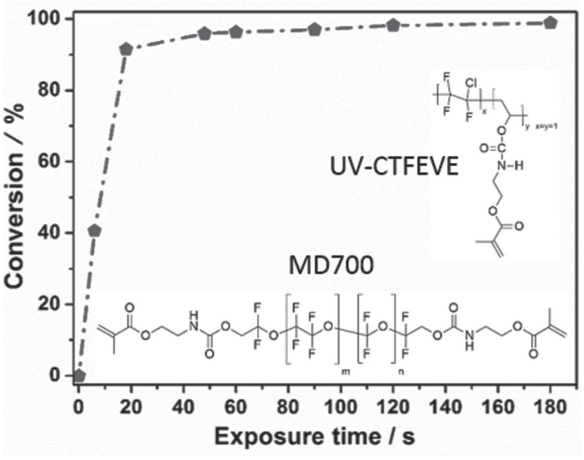

Figure 5. Conversion curve of the UV-curing process for the UV-CTFEVE/MD700 system, as obtained from UV-DSC measurements. The molecular structures of UV-CTFEVE and MD700 polymers are given as insets.

binder, thus resulting in improved cleanability of the deposited coating. A preliminary analysis was conducted on the composition of the XL-coating precursor to evaluate the optimal UV-CTFEVE:MD700 ratio. After visual inspection, it was found that for concentrations of MD700 exceeding 2 wt%, the reactive mixture (and the resulting XL-coating) became turbid white with the presence of some precipitate in the precursor solution. This behavior was ascribed to phase segregation of the two polymeric components that may occur as a result of the poor miscibility of PFPE and UV-CTFEVE. Accordingly, a 98:2 = UV-CTFEVE:MD700 weight ratio was employed for the preparation of the XL-coating.

In order to monitor the kinetics of the UV-curing process, photocalorimetric (UV-DSC) measurements were performed on the coating material preirradiated with UV light for increasing exposure times. As shown in Figure 5, where the conversion curve for the XL-coating is presented, the UV-curing reaction reaches a conversion of over 98% already after 60 s of UV exposure, thus further confirming the extreme rapidity and high efficiency of this photochemical approach that proves particularly interesting in view of its potential upscalability to large production volumes.

DSC measurements were performed on the fully UV-cured system to evaluate the thermal transitions of the XL-coating. As presented in **Figure 6**A, the coating shows a clear biphasic behavior, evidenced by the presence of two distinct second-order transitions ascribable to the nanoscale segregation of the PFPE and the urethane phases resulting from their different solubility parameters.[23] A first low-temperature T_g is found at –60 °C which can be ascribed to the soft fluorinated segments. On the contrary, the higher T_g found at above room temperature (37 °C) is associated with the hydrogenated urethane phase. Moreover, no crystallization phenomena are observed in the UV-cured material. These characteristics make this system suitable for outdoor use.

The thermo-oxidative stability of the UV-cured XL-coating was evaluated by means of TGA in air, and the results are shown in Figure 6B. A first mass loss of about 10%–15% is observed in the 100–250 °C temperature range that may be ascribed to the breaking of the urethane bonds in the XL-coating. At higher temperatures (250–450 °C), another 60% mass loss event occurs, which can be related to the thermal cleavage of the acrylic groups. For temperatures higher than 450 °C, a final mass loss event is observed that takes into account the degradation of the PFPE moiety accompanied by the complete decrosslinking of the polymeric system.[24] Temperatures of 152, 198, and 374 °C are found for 5%, 10%, and 50% mass losses, respectively, further confirming the excellent thermo-oxidative stability of the new XL-coating, as well as its applicability under real outdoor conditions. A similar behavior was also observed in N_2 environment (see Figure S4 in the Supporting Information).

To evaluate the surface wettability and the resulting cleanability of the XL-coating, static contact angle measurements were performed using water and diiodomethane as probe liquids. The surface tension γ of the coating with its dispersive and polar components (γ^d and γ^p, respectively) was then estimated from contact angle measurements using the Wu method.[25] The highly hydrophobic and moderately oleophobic character of the XL-coating is evidenced by the measured contact angles against water (θ_{H2O} = 111.0°) and diiodomethane (θ_{CH2I2} = 91.0°), resulting from the low value of surface tension of the coating (γ = 18.0 mN m^{-1}, γ^d = 15.3 mN m^{-1}, and γ^p = 2.7 mN m^{-1}) (**Figure 7**A,B). Clearly, compared to bare uncoated glass (θ_{H2O} = 12.7°, θ_{CH2I2} = 58.6°, γ = 71.7 mN m^{-1},

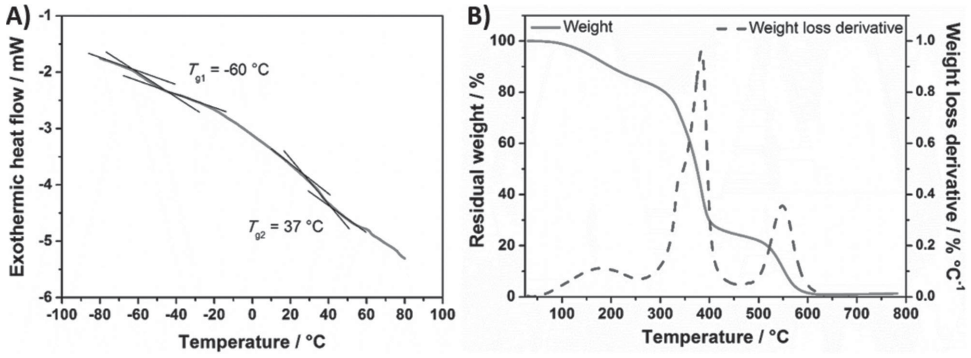

Figure 6. A) DSC trace and B) TGA thermogram of the UV-CTFEVE/MD700-based XL-coating.

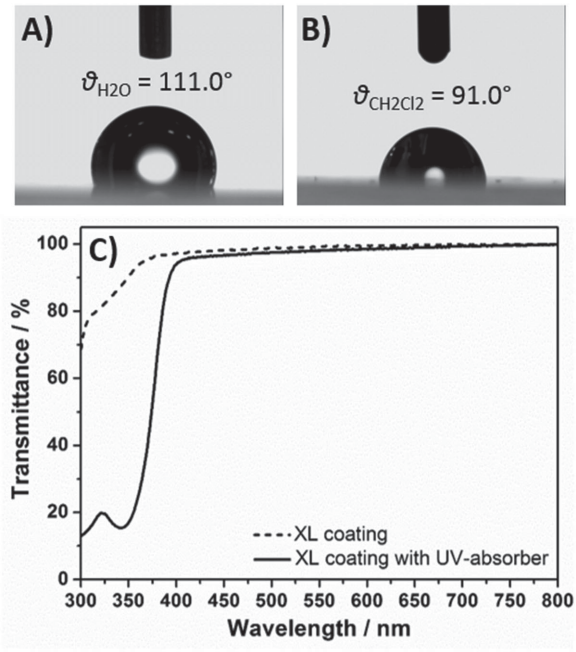

Figure 7. A) Water (θ_{H2O}) and B) diiodomethane (θ_{CH2I2}) static contact angles on the XL-coating. C) Transmittance spectra of the XL-coating without and with the addition of the UV absorber.

$\gamma^d = 27.3$ mN m^{-1}, and $\gamma^p = 44.4$ mN m^{-1}), the application of this new fluorinated XL-coating significantly improves the cleanability of the external side of the photoanode in the PECD. Indeed, it prevents physical barriers for the incident solar photons (e.g., soil, dust, water drops, etc.) to deposit onto it, thus potentially leading to extended device lifetime during outdoor operation. In addition, the introduction of the perfluorinated moiety (PFPE) in the UV-curable coating formulation allows to significantly decrease the wettability of the new XL-coating with respect to recently published results on a similar system,[14,21] thus further boosting its characteristics of ready cleanability.

In view of its practical application as protective coating onto PECDs, the optical properties of the XL-coating are of critical importance. In particular, a high transmittance over the entire visible spectrum must be guaranteed, so as to prevent undesirable absorption of incident solar photons that would inevitably reduce device performance. As shown in Figure 7C, where the UV–vis transmission spectrum of the XL-coating is shown, no parasitic absorptions in the 350–800 nm wavelength range are observed (below 350 nm, the contribution to absorption from the photoinitiator can be observed). In particular, despite the heterogeneous nature of this system as inferred from DSC analysis, the new UV-curable coating appears highly transparent (transmittance over 99%), clearly indicating that the phase segregation between fluorinated and urethane moieties is in the submicrometric range, in accordance with the published literature.[26] These results confirm the excellent optical transparency of the new fluorinated UV-curable material.

Due to the presence of light sensitive materials (e.g., electrolyte additives, N719 dye, etc.) that may undergo photo-oxidative degradation during prolonged exposure to the high-energy UV component of the solar spectrum, a strategy to prevent or limit such UV photons from reaching the sensitive components in the PECD stack would be highly desirable as this may further prolong its operational lifetime. To this end, a hydroxyphenylbenzotriazole-based UV absorber (Tinuvin 1130, CIBA—see Figure S5 in the Supporting Information for the molecular structure) was added to the XL-coating formulation to provide the new fluorinated system with an extra UV-screening functionality. As shown in Figure 7C, the addition of such UV absorber significantly increases the absorption in the wavelength region below 400 nm without minimally affecting the optical properties of the XL-coating in the visible range.

In order to ascertain the effect of the proposed functional coating on the PECD performance, a long-term weathering study was conducted under real outdoor conditions for a period of three months. To the best of our knowledge, this represents the first demonstration of a prolonged stability test on PECDs upon actual outdoor exposure. The aging test was performed on three devices: a PECD assembled with the standard liquid electrolyte; a second PECD incorporating the newly proposed quasi-solid polymer electrolyte; a third PECD including both the quasi-solid polymer electrolyte and the functional fluoropolymeric coating proposed in this work. The three PECDs were uninterruptedly exposed for three months (day and night) on top of the roof of the Politecnico di Torino building in Turin (45°06′34.6″N, 7°66′13.5″E), located in the north-western end of Italy in a humid subtropical climate zone. The highly variable climatic conditions of Turin are particularly useful to carry out a realistic study of device aging. As shown in **Figure 8**D, outdoor temperatures ranged from 8 to 36 °C during the second quarter of 2015 (between June and August) and 37 precipitation phenomena (e.g., rain, storm, hail) were recorded by the local meteorological station.[27] The transmittance of the PECD in the colored and bleached states was recorded every 2 d, and the resulting trends are shown in Figure 8. In the considered period, the liquid-state PECD showed both a marked reduction of the coloration degree and a lowered efficiency of the bleaching phenomenon (Figure 8A). Such behavior may be primarily ascribed to the volatility of the acetonitrile-based liquid electrolyte, but the deposition of dirt on the front electrode as well as the effect of the UV radiation present in sunlight during outdoor operation may also play a significant role. The aging behavior of the quasi-solid PECD assembled with the newly-designed polymer electrolyte membrane is shown in Figure 8B. In this case, improved stability of the PECD transmittance in the colored state was reported compared to the liquid-based PECD. This behavior likely indicates that no electrolyte leakage occurred for the quasi-solid PECD and that the insertion of Li^+ ions in the WO_3 layer proceeded efficiently during the whole operating period. On the other hand, a slight reduction of the transmittance associated with the bleached stated is recorded after the initial 30 d. This phenomenon cannot be attributed to the volatilization of the electrolyte, as this would have also led to a variation of PECD transmittance in the colored state. Conversely, we primarily ascribe this behavior to the accumulation of dirt and dust onto the front electrode glass after the initial three–four weeks of outdoor exposure. In addition to that, a second minor contribution may be given by oxidative photodegradation phenomena promoted by the UV component of sunlight, the latter being very

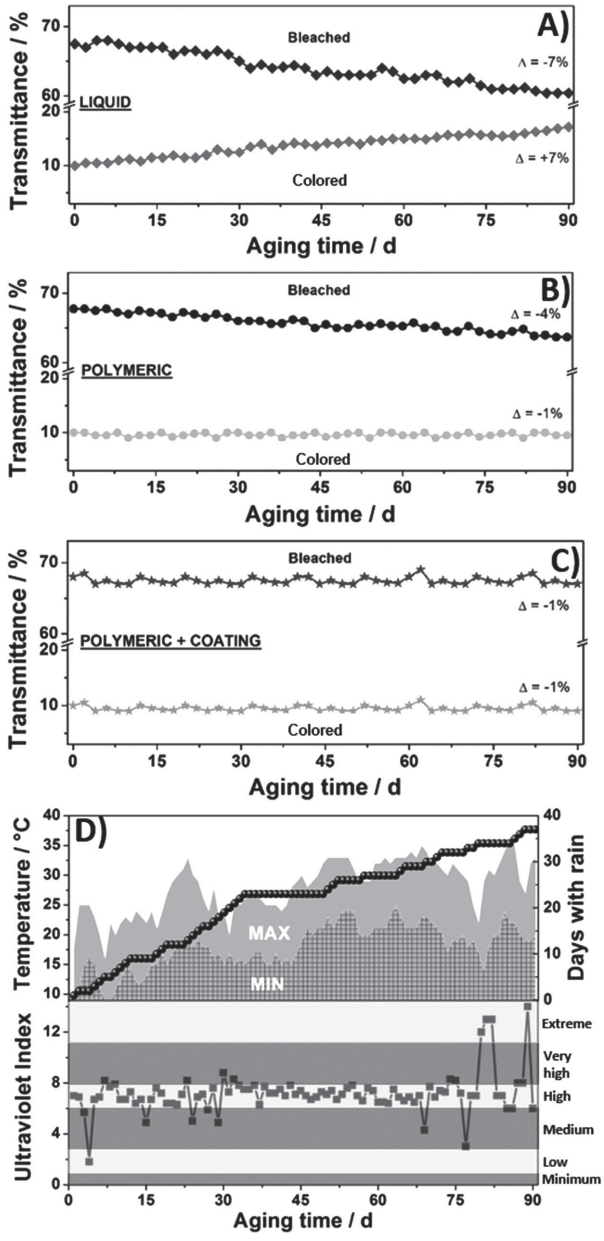

Figure 8. Outdoor aging tests carried out on three different PECDs: A) liquid-state, B) polymeric uncoated, and C) polymeric coated. The shown transmittance values in the colored and bleached states were recorded every 2 d for a period of three months. D) Minimum and maximum temperatures recorded in Turin (Italy) during the aging test, along with the number of precipitation phenomena (i.e., the number of raining days) and the UV index recorded by the local meteorological station.

intense during the period chosen to carry out the aging test (Figure 8D).[28] These photoinduced processes (partly catalyzed by the presence of TiO_2 in the front electrode) cause a slight yellowing of the device (see Figure S6 in the Supporting Information), likely due to the degradation of some of the polymer electrolyte components. These detrimental processes appear to be significantly reduced when the XL-coating is incorporated

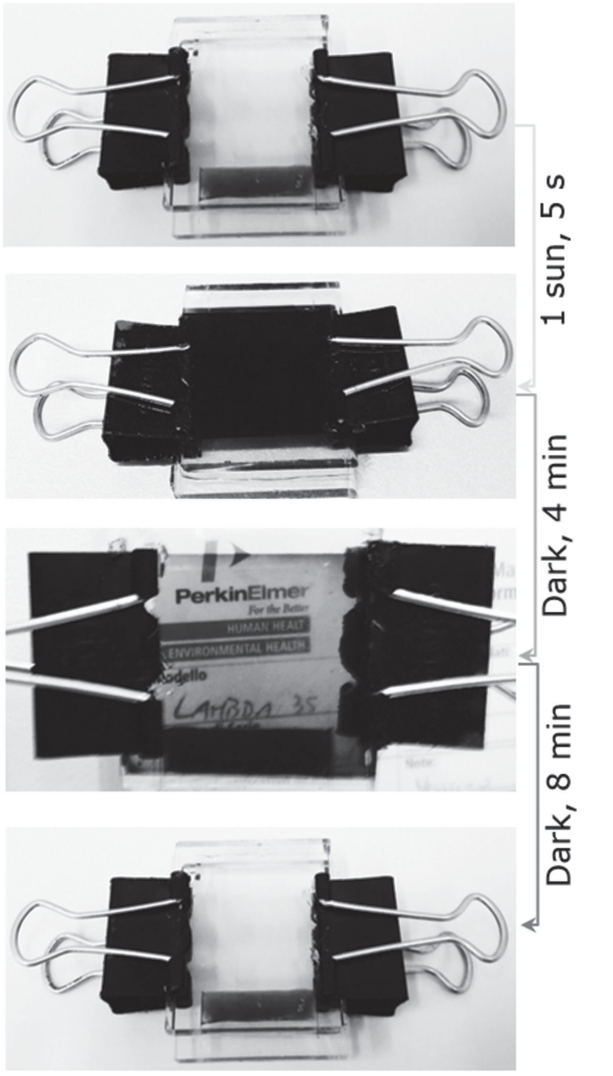

Figure 9. Coloration/bleaching of the PECD assembled with the quasi-solid polymer electrolyte membrane and the self-cleaning/UV-cutting fluorinated coating. Photographs were taken after 90 d of outdoor exposure.

in the PECD system. As shown in Figure 8C, in this latter case both transmittance values (e.g., bleached and colored states) are kept constant for the whole aging study. These results demonstrate the effective protective action of the photopolymerized fluorinated coating in terms of both easy cleanability and UV shielding. As evidenced by visual inspection after 90 d of continuous outdoor exposure, the quasi-solid PECD system incorporating the XL-coating fully retained its complete coloration/bleaching functionality (**Figure 9**).

3. Conclusion

Light-cured polymeric components were proposed for the first time for the manufacture of efficient and highly durable quasi-solid PECDs. The liquid electrolyte was replaced by a flexible quasi-solid polymer electrolyte membrane, thermally and

mechanically stable, able to trap the redox couple necessary for the functioning of the DSSC and the Li^+ ions for the coloration/bleaching process of the ECD. A further step toward a stable device under real outdoor conditions involved the application of a photocurable fluoropolymeric thin coating film on the external glass-side of the PECD. This coating proved to be effective both as easily cleanable layer (preventing water and soil particles from depositing onto the PECD front electrode during exposure to urban outdoor conditions) and UV-blocking layer useful to avoid UV-induced photo-oxidative degradation phenomena typically encountered in hybrid organic/inorganic devices when continuously exposed to sunlight. The PECD assembled by combining these light-cured polymer-based components and inorganic thin films demonstrated excellent device operation, in some cases higher than the liquid-based counterpart. In addition, these newly-developed materials allowed to achieve a remarkably stable performance during prolonged aging tests performed under real outdoor conditions. The results of this study open the way to a new generation of thermally, electrochemically, and photochemically stable polymer-based PECDs, demonstrating for the first time their true potential as readily upscalable smart windows for modern energy-saving buildings.

4. Experimental Section

Materials: Tungsten oxide (WO_3) powder (99.99%), nitric acid (HNO_3), Triton X-100, absolute ethanol, BEMA (average M_n: 1700), PEGMA (average M_n: 700), LiI, iodine (I_2), acetonitrile (ACN) chloroform ($CHCl_3$), hexachloroplatinic acid solution (H_2PtCl_6, 8 wt% in H_2O), and di-*n*-butyltin dilaurate (DBTDL) were purchased from Sigma-Aldrich. Titanium dioxide (TiO_2) nanopowder (Degussa P25) was kindly provided by Evonik. The ruthenium complex dye (N719) and conductive glasses (FTO, sheet resistance 12–14 Ω sq^{-1}, 82%–84% transmittance in the visible) were purchased from Dyesol. 2-hydroxy-2-methyl-1-phenyl-1-propanone (Irgacure 1173) was purchased from BASF. The CTFEVE polymeric binder Lumiflon LF-910LM was purchased from Asahi Glass Company Ltd. 2-isocyanatoethyl methacrylate (IEM) was obtained from Showa Denko K.K. The difunctional methacrylic PFPE oligomer Fluorolink MD700 was kindly provided by Solvay Specialty Polymers. The hydroxyphenyl-benzotriazole-based UV-absorber (Tinuvin 1130, in this article referred to as TIN) was kindly provided by Ciba Specialty Chemicals.

Fabrication and Characterization of the Electrodes: WO_3 films on FTO glasses were prepared by electron beam gun evaporation at room temperature, at a pressure of 10^{-5} mbar in a vacuum chamber evacuated by a turbomolecular and a mechanical pump. A quartz thickness controller was used for the deposition of the desired film thickness. Subsequently, a TiO_2 film was deposited on top of the WO_3 layer by doctor blading a TiO_2 paste, covering a fraction of the WO_3 area equal to 15% (on the bottom area, by using a mask).[5,20] The TiO_2 paste was prepared starting from 3 g of Degussa P25, which was ground in a porcelain mortar with a small amount (0.7 mL) of HNO_3 1.5 M. The resulting viscous paste was further diluted by gradual addition of distilled water under continuous grinding (0.5 mL each time), until the density of the paste reached the value of 1.5 g mL^{-1}. Approximately 4–5 mL of distilled water was used to reach the desired density value. Finally, five drops of a detergent (Triton X-100) were added to facilitate the spreading of the paste on the WO_3 film.[29] After ≈40 min of continuous grinding, the paste was put into an ultrasonic bath for 6 min. The ultrasonic bath was used to further break down the large aggregates of TiO_2 nanoparticles as well as to enhance the homogeneity of the paste.[29a] The prepared WO_3/TiO_2 films were dried at 100 °C for 40 min and sensitized by dipping while they were still hot (at about 80 °C) in a 0.3×10^{-3} M ethanol solution of N719, overnight. Only the part of the film covered with TiO_2 was dipped inside the dye solution, even though the dye is preferentially adsorbed on the surface of TiO_2 rather than on WO_3.[30] Upon extraction from the solution, the samples were thoroughly rinsed with methanol to remove the excess dye.

Electrodes' thickness was measured ex situ by an Ambios XP-1 stylus profilometer. The overall morphology of the prepared samples was investigated by field emission SEM (ZEISS Supra 40).

Counter electrodes were prepared by electrodeposition from an aqueous hexachloroplatinic acid solution (H_2PtCl_6, 8 wt% in H_2O). A three-electrode configuration was used: an FTO glass was used as the working electrode, an Ag/AgCl electrode served as the reference and a Pt wire as the counter electrode, respectively. The electrodeposition process was carried out at a constant current of 0.5 mA cm^{-2} for 15 s, in order to prepare transparent counter electrodes. The resulting Pt films consisted of distinct Pt nanoparticles with high surface area, ensuring an efficient catalytic activity.[5,31]

Preparation and Characterization of the Polymer Electrolyte Membrane: Photocured polymer membranes were prepared using the oligomers BEMA and PEGMA in the 30:70 weight ratio, while Irgacure 1173 (2 wt%) was added as the free-radical photoinitiator. The resulting viscous liquid reactive mixture was sandwiched between two UV-transparent glasses, separated by a 100 μm thick tape. Self-standing membranes were obtained by UV irradiating the mixtures for 2 min using a medium vapor pressure Hg lamp (Helios Italquartz, Italy), with an irradiation intensity at the surface of 30 mW cm^{-2}, measured with a UV Power Puck II radiometer (EIT).

The kinetics of the photopolymerization reaction was determined by RT-FTIR spectroscopy, employing a Thermo-Nicolet 5700 instrument. The reactive mixture was deposited over silicon wafers in the form of a thin layer, and exposed concurrently to UV beam (which induces the polymerization) and IR beam (which analyzes in situ the extent of the reaction). The conversion of the methacrylate double bonds at a given time was calculated by monitoring the peak area under the 1634 cm^{-1} band (methacrylate C = C stretching signal), normalized by a stable signal in the spectra (C = O stretching peak at 1726 cm^{-1}). The gel content (insoluble crosslinked fraction) of the UV-cured polymer membranes was determined by measuring the weight loss after 24 h of extraction in chloroform at ambient temperature (standard test method ASTM-D2765-11).

The glass transition temperature (T_g) was evaluated by DSC with a DSC 204 F1 Phoenix (Netzsch) instrument in the temperature range between −70 and +70 °C, at a heating rate of 10 °C min^{-1}, under N_2 flux. The thermal traces were recorded after a heating/cooling cycle, useful to cancel the thermal history of the polymer samples. The thermal stability was tested by TGA under N_2 flux, with a TG 209 F1 Libra instrument from Netzsch, in the temperature range of 25–600 °C at a heating rate of 10 °C min^{-1}.

To be used as electrolytes, the crosslinked polymer membranes were activated by a rapid 3 min soaking in an acetonitrile solution containing LiI 0.50 M, I_2 5.0×10^{-3} M, and TBP 0.50 M.

Preparation and Characterization of the Polymeric Self-Cleaning Protective Coating: To obtain the photocurable self-cleaning/UV-absorbing coating two distinct polymeric precursors were employed, namely, a CTFEVE-based UV-curable polymer (in this article referred to as UV-CTFEVE) and MD700. For the preparation of UV-CTFEVE, Lumiflon LF-910LM was reacted with IEM in the presence of DBTDL according to a procedure described elsewhere,[14,21] to produce a fluorinated polymer with pendant methacrylate groups linked to the fluoropolymeric backbone by means of urethane bonds. UV-CTFEVE was then mixed with MD700 in the 98:2 = UV-CTFEVE:MD700 weight ratio followed by the addition of $CHCl_3$ as diluting solvent (30 wt% total dry), Irgacure 1173 (3 wt%) as radical photoinitiator, and TIN (2 wt%) as UV absorber. The reactive precursor mixture was then allowed to magnetically stir in the dark overnight prior to deposition. The final UV-cured fluoropolymeric coating (XL-coating) was obtained by spin-casting (1000 rpm, 30 s on a SPIN150 spin coater, SPS-Europe) such reactive mixture on the outer side of the PECD photoanode and, immediately after, irradiating it in a nitrogen atmosphere with a medium pressure mercury lamp equipped with an optical guide (Lightningcure LC8, Hamamatsu) for 60 s under an irradiation intensity of 25 mW cm^{-2} (measured with the Power Puck II radiometer). A final film thickness of 10 μm was obtained, as measured by optical profilometry (Microfocus, UBM).

The reaction kinetics of the UV-curing process was monitored by means of in situ photocalorimetric (UV-DSC) measurements performed on a DSC/823e (Mettler Toledo) coupled to a fiber-guided UV light source in the 300–450 nm wavelength range at an intensity of 15 mW cm^{-2} generated by a medium-pressure mercury lamp (Lightningcure LC8, Hamamatsu). Samples of the UV-curable precursor mixture (≈5–10 mg) were placed into an open aluminum crucible and pre-exposed to such UV light at 25 °C under nitrogen flow (50 mL min^{-1}) for a given time t (up to 180 s). Then, UV-DSC was performed on each pre-exposed sample to measure the residual heat of reaction at UV-exposure time t ($\Delta H_{res}(t)$) as the integral of the resulting exothermic curve. Finally, the values of $\Delta H_{res}(t)$ at different UV pre-exposure times were normalized to the heat of reaction of the uncured mixture (ΔH^0), to build the conversion curve. The conversion of the UV-curing reaction was calculated according to Equation (1)

$$\text{Conversion}(\%) = \left(1 - \frac{\Delta H_{res}(t)}{\Delta H^0}\right) \cdot 100 \tag{1}$$

The T_g of the coating material was obtained from calorimetric measurements (DSC) on fully crosslinked solid state samples using a Mettler-Toledo DSC/823e instrument at a scan rate of 20 °C min^{-1} under N_2 flux. Values of T_g were obtained from the second heating ramp.

TGA measurements were performed on fully crosslinked solid state samples by means of a Q500 TGA system (TA Instruments) from ambient temperature to 800 °C at a scan rate of 10 °C min^{-1} both in air and under flowing N_2.

Static optical contact angle (OCA) measurements were performed on the fully crosslinked XL-coating at room temperature using an OCA 20 (Data Physics) equipped with a CCD photocamera and with a 500 µL Hamilton syringe to dispense liquid droplets. The reported results were obtained from the average of a minimum of 25 measurements taken in different regions of the surface of the UV coating. Water (H_2O) and diiodomethane (CH_2I_2) were used as probe liquids.

UV–vis absorption spectra were recorded in air at room temperature in transmission mode by means of an Evolution 600 UV–vis spectrophotometer (Thermo Scientific). The XL-coating (with and without TIN as UV-absorbing agent) was formed on quartz substrates by spin-coating (WS-400B-NPP Spin-Processor, Laurell Technologies Corp.) the precursor solution at 1200 rpm for 40 s in air followed by UV-curing in N_2.

Assembly and Characterization of the PECDs: PECDs with typical dimensions of 2.5 × 3.0 cm^2 were prepared as follows: the sensitized FTO/WO_3/TiO_2/N719 photoanode and the Pt/FTO counter electrode were faced one in front of the other, slightly displaced along their longitudinal axis in order to preserve enough space for electrical contacts. The 100 µm thick polymer electrolyte membrane, obtained by proper activation with the redox mediator, was placed onto the anode surface and covered with the counter electrode. The resulting device was held together by clamps and sealed peripherally by means of an epoxy glue. Measurements followed immediately.

The coloration of the devices was performed under open circuit conditions, upon exposure to a 1000 W m^{-2} visible irradiation for various time intervals, by means of an ORIEL 96000 solar simulator with a AM 1.5G filter. The incident irradiance was measured by a Si photodiode (VTB8440B) calibrated against a Melles Griot 13PE001 broadband power meter.[29a] The maximum time used for the complete coloration of the devices was 12 min. The bleaching of the devices was performed under dark in short-circuit conditions, for a maximum time of 12 min.

From the transmittance spectra (recorded with a spectrophotometer Lambda 35, PerkinElmer) the luminous transmittance was calculated by Equation (2)[32]

$$T_{lum} = \frac{\int_{350\ nm}^{750\ nm} f(\lambda) \cdot T(\lambda) d\lambda}{\int_{350\ nm}^{750\ nm} f(\lambda) d\lambda} \tag{2}$$

with $f(\lambda)$ being the relative sensitivity of the human eye in the photopic state and $T(\lambda)$ the measured transmittance spectrum.

PhCE, given by Equation (3), was calculated immediately after device assembly[5,20]

$$\text{PhCE} = \frac{\Delta OD_{lum}}{G_T \cdot t} = \frac{\log^{T_{lum,bleached}/T_{lum,\ colored}}}{G_T \cdot t} \left[\text{cm}^2\ \text{min}^{-1}\ \text{W}^{-1}\right] \tag{3}$$

with G_T being the total solar intensity for incidence normal to the device (in W cm^{-2}) and t the exposure time (in minutes). The units were thus chosen, so as to get values in the order of one for PhCE, as is expected for an efficiency index. $T_{lum,\ bleached}$ and $T_{lum,\ colored}$ are the luminous transmittance in the bleached and colored state, respectively, given by Equation (2).

Characteristic *I–V* curves of the PECDs were taken using the aforementioned solar simulator, in conjunction with a Keithley 236 source meter. *I–V* curves were taken after 60 s of illumination, to avoid coloration of the devices before optical measurements.

Aging tests under real outdoor weathering conditions were carried out by placing the PECDs on top of the roof of the Politecnico di Torino building in Turin (45°06′34.6″N, 7°66′13.5″E) for three months and monitoring their bleaching/colored-state transmittance every 2 d. When exposed, devices were kept colored under open-circuit conditions.

Supporting Information

Supporting Information is available from the Wiley Online Library or from the author.

Received: September 5, 2015
Revised: November 4, 2015
Published online: December 28, 2015

[1] a) K. Wang, H. Wu, Y. Meng, Y. Zhang, Z. Wei, *Energy Environ. Sci.* **2012**, *5*, 8384; b) D. Ge, E. Lee, L. Yang, Y. Cho, M. Li, D. S. Gianola, S. Yang, *Adv. Mater.* **2015**, *27*, 2489; c) M. H. Yeh, L. Lin, P. K. Yang, Z. L. Wang, *ACS Nano* **2015**, *9*, 4757.

[2] a) P. Gomez-Romero, *Adv. Mater.* **2001**, *13*, 163; b) C. Bechinger, S. Ferrere, A. Zaban, J. Sprague, B. A. Gregg, *Nature* **1996**, *383*, 608; c) Z. Jiao, J. L. Song, X. W. Sun, X. W. Liu, J. M. Wang, L. Ke, H. V. Demir, *Sol. Energy Mater. Sol. Cells* **2012**, *98*, 154.

[3] a) I. Y. Jeon, M. J. Ju, J. Xu, H. J. Choi, J. M. Seo, M. J. Kim, I. T. Choi, H. M. Kim, J. C. Kim, J. J. Lee, H. K. Liu, H. K. Kim, S. Dou, L. Dai, J. B. Baek, *Adv. Funct. Mater.* **2015**, *25*, 1170; b) V. M. Blas-Ferrando, J. Ortiz, V. González-Pedro, R. S. Sánchez, I. Mora-Serõ, F. Fernández-Lázaro, A. Sastre-Santos, *Adv. Funct. Mater.* **2015**, *25*, 3220; c) J. Jensen, M. Hösel, A. L. Dyer, F. C. Krebs, *Adv. Funct. Mater.* **2015**, *25*, 2073; d) H. J. Yen, C. J. Chen, G. S. Liou, *Adv. Funct. Mater.* **2013**, *23*, 5307; e) J. Lin, X. Liu, S. Zhu, X. Chen, *Nanotechnol. Rev.* **2015**, *4*, 209; f) G. Wang, W. Xiao, J. Yu, *Energy* **2015**, *86*, 196; g) Z. Seidalilir, R. Malekfar, H. P. Wu, J. W. Shiu, E. W. G. Diau, *ACS Appl. Mater. Interfaces* **2015**, *7*, 12731; h) R. Adel, T. Abdallah, Y. M. Moustafa, A. M. Al-Sabagh, H. Talaat, *Superlattices Microstruct.* **2015**, *86*, 62; i) N. Chander, A. F. Khan, V. K. Komarala, *RSC Adv.* **2015**, *5*, 66057; j) S. Shalini, R. Balasundara Prabhu, S. Prasanna, T. K. Mallick, S. Senthilarasu, *Renewable Sustainable Energy Rev.* **2015**, *51*, 1306; k) R. Y. Y. Lin, F. L. Wu, C. T. Li, P. Y. Chen, K. C. Ho, J. T. Lin, *ChemSusChem* **2015**, *8*, 2503.

[4] a) A. Cannavale, G. E. Eperon, P. Cossari, A. Abate, H. J. Snaith, G. Gigli, *Energy Environ. Sci.* **2015**, *8*, 1578; b) M. C. Yang, H. W. Cho,

J. J. Wu, *Nanoscale* **2014**, *6*, 9541; c) F. Malara, A. Cannavale, S. Carallo, G. Gigli, *ACS Appl. Mater. Interfaces* **2014**, *6*, 9290; d) E. Amasawa, N. Sasagawa, M. Kimura, M. Taya, *Adv. Energy Mater.* **2014**, *4*, 1400379.

[5] G. Leftheriotis, G. Syrrokostas, P. Yianoulis, *Sol. Energy Mater. Sol. Cells* **2012**, *96*, 86.

[6] S. Yang, J. Zheng, M. Li, C. Xu, *Sol. Energy Mater. Sol. Cells* **2012**, *97*, 186.

[7] G. De Filpo, S. Mormile, F. P. Nicoletta, G. Chidichimo, *J. Power Sources* **2010**, *195*, 4365.

[8] B. N. Reddy, R. Mukkabla, M. Deepa, P. Ghosal, *RSC Adv.* **2015**, *5*, 31422.

[9] L. Hechavarría, N. Mendoza, M. E. Rincón, J. Campos, H. Hu, *Sol. Energy Mater. Sol. Cells* **2012**, *100*, 27.

[10] C. H. Wu, C. Y. Hsu, K. C. Huang, P. C. Nien, J. T. Lin, K. C. Ho, *Sol. Energy Mater. Sol. Cells* **2012**, *99*, 148.

[11] F. Pichot, S. Ferrere, R. J. Pitts, B. A. Gregg, *J. Electrochem. Soc.* **1999**, *146*, 4324.

[12] U. O. Krašovec, A. Georg, A. Georg, V. Wittwer, J. Luther, M. Topič, *Sol. Energy Mater. Sol. Cells* **2004**, *84*, 369.

[13] F. Bella, C. Gerbaldi, C. Barolo, M. Grätzel, *Chem. Soc. Rev.* **2015**, *44*, 3431.

[14] F. Bella, G. Griffini, M. Gerosa, S. Turri, R. Bongiovanni, *J. Power Sources* **2015**, *283*, 195.

[15] a) J. V. Crivello, E. Reichmanis, *Chem. Mater.* **2014**, *26*, 533; b) J. Shao, Y. Huang, Q. Fan, *Polym. Chem.* **2014**, *5*, 4195; c) C. Dietlin, S. Schweizer, P. Xiao, J. Zhang, F. Morlet-Savary, B. Graff, J. P. Fouassier, J. Lalevée, *Polym. Chem.* **2015**, *6*, 3895.

[16] S. Papaefthimiou, G. Leftheriotis, P. Yianoulis, *Solid State Ionics* **2001**, *139*, 135.

[17] a) A. Sacco, F. Bella, S. De La Pierre, M. Castellino, S. Bianco, R. Bongiovanni, C. F. Pirri, *ChemPhysChem* **2015**, *16*, 960; b) J. R. Nair, L. Porcarelli, F. Bella, C. Gerbaldi, *ACS Appl. Mater. Interfaces* **2015**, *7*, 12961; c) S. J. Seo, H. J. Cha, Y. S. Kang, M. S. Kang, *Electrochim. Acta* **2015**, *173*, 425; d) F. Bella, A. Sacco, G. Massaglia, A. Chiodoni, C. F. Pirri, M Quaglio, *Nanoscale* **2015**, *7*, 12010.

[18] a) H. Kim, S. J. Lee, *Adv. Funct. Mater.* **2015**, *25*, 4496; b) C. Yao, Z. Liu, C. Yang, W. Wang, X. J. Ju, R. Xie, L. Y. Chu, *Adv. Funct. Mater.* **2015**, *25*, 2980.

[19] G. Syrrokostas, G. Leftheriotis, P. Yianoulis, *Solid State Ionics* **2015**, *277*, 11.

[20] G. Leftheriotis, G. Syrrokostas, P. Yianoulis, *Solid State Ionics* **2013**, *231*, 30.

[21] G. Griffini, F. Bella, F. Nisic, C. Dragonetti, D. Roberto, M. Levi, R. Bongiovanni, S. Turri, *Adv. Energy Mater.* **2015**, *5*, 1401312.

[22] a) G. Griffini, M. Levi, S. Turri, *Prog. Org. Coat.* **2014**, *77*, 528; b) G. Griffini, M. Levi, S. Turri, *Sol. Energy Mater. Sol. Cells* **2013**, *118*, 36; c) J. Scheirs, *Modern Fluoropolymers: High Performance Polymers for Diverse Applications*, John Wiley & Sons Ltd, Chichester, UK **1997**.

[23] D. Molina, G. Griffini, M. Levi, S. Turri, *Polym. Adv. Technol.* **2014**, *25*, 1082.

[24] R. Bongiovanni, A. Medici, A. Zompatori, S. Garavaglia, C. Tonelli, *Polym. Int.* **2012**, *61*, 65.

[25] S. Wu, *J. Colloid Interface Sci.* **1979**, *71*, 605.

[26] A. Priola, R. Bongiovanni, G. Malucelli, A. Pollicino, C. Tonelli, G. Simeone, *Macromol. Chem. Phys.* **1997**, *198*, 1893.

[27] IL METEO.IT, http://www.ilmeteo.it (accessed: August **2015**).

[28] Meteo Piateda, http://www.meteopiateda.it/ (accessed: August **2015**).

[29] a) G. Syrrokostas, G. Leftheriotis, P. Yianoulis, *Renewable Energy* **2014**, *72*, 164; b) G. Syrrokostas, M. Giannouli, P. Yianoulis, *Renewable Energy* **2009**, *34*, 1759; c) D. Zhang, J. A. Downing, F. J. Knorr, J. L. McHale, *J. Phys. Chem. B* **2006**, *110*, 21890.

[30] A. Hauch, A. Georg, U. Opara Krašovec, B. Orel, *J. Electrochem. Soc.* **2002**, *149*, H159.

[31] G. Syrrokostas, A. Siokou, G. Leftheriotis, P. Yianoulis, *Sol. Energy Mater. Sol. Cells* **2012**, *103*, 119.

[32] G. Leftheriotis, G. Syrrokostas, P. Yianoulis, *Sol. Energy Mater. Sol. Cells* **2010**, *94*, 2304.